Extracting a Bias-Dependent Large Signal MESFET Model from Pulsed *I/V* Measurements

Tomás Fernández, Yolanda Newport, José M. Zamanillo, Antonio Tazón, *Member, IEEE*, and Angel Mediavilla, *Member, IEEE*

***Abstract*—In this paper a new large-signal metal semiconductor field effect transitor (MESFET) model suitable for applications to nonlinear microwave CAD has been developed and the different phenomena involved in the nonlinear behavior of the transistor have been studied. The importance of this work lies in the fact that multibias starting points (hot and cold device) for pulsed measurements are used to derive a single expression for I_{ds} that describes the dc as well as the small and large signal behavior of the transistor, while taking into account the quiescent point dependence. The algorithms of this new model can easily be incorporated into commercially available nonlinear simulators. The operating-point dependent current I_{ds} is modeled by two nonlinear sources: one of them is the dc characteristic nonlinear equation, and the other represents the differences between dc and pulsed characteristics at every bias point. A complete large-signal model is presented for a 10 * 140 μm GaAs-MESFET chip (F20 process) from the GEC-MARCONI Foundry and a 16 * 250 μm MESFET chip (DIOM process) from the Siemens Foundry. Comparisons have been made between simulations and measurements of pulsed characteristics at different operating points. There was very good agreement between the P_{in}/P_{out} measurements and the MDS simulations using the complete large signal model.**

I. Introduction

MODERN communications systems require more and more sophisticated microwave integrated circuits (MIC) and monolithic microwave/millimeter-wave integrated circuits (MMIC) making it necessary to develop accurate models for large-signal devices. Furthermore, the increasing integration of the monolithic circuit has reinforced the need of such models in order to minimize the number of design and fabrication cycles required. Therefore, it is very important for nonlinear software tools to have large-signal models which take into account phenomena such as trap effects, heating, noise, etc.

The most common way of modeling the nonlinear equation of the channel current is to extract the parameters of this equation from the dc characteristics and the S parameters in the frequency band of interest at several operating points (quasi-static approximation) [1]–[3]. Another way involves using pulsed characteristics [4], [5]. This method is only valid at a given operating point and provides a better simulation of the actual operation of the transistor because it takes heating into account. However, none of these approaches reliably predicts the behavior of the transistor because they do not take into consideration low-frequency dispersion, dc operation, or thermal phenomena, all of which affect the dynamic characteristics. Recently, several authors have proposed improved models that use a second nonlinear current source [6], [7], and [15]. These models are able to predict the low-frequency dispersion but do not take into account the dependence of the model parameters on the operating-point or the problem of pulsed measurements.

In order to develop a complete nonlinear device model it is necessary to determine the different phenomena involved in the nonlinear behavior of the transistor. In Section II, we will demonstrate the importance of pulsed measurements and the influence of the operating point on the behavior of MESFET's. In the Section III, a very useful current source model is developed that takes into consideration the real heating (the operating point dependence). This current I_{ds} is modeled by two nonlinear sources: one of them simulates the dc characteristics and the other represents the large-signal RF behavior at every bias point. This model is also capable of simulating the low-frequency dispersion, taking into account the heating of the transistor. The main aim of the equation developed is to model large-signal GaAs-MESFET's with CAD-oriented circuit topology, starting from their drain and gate-pulsed characteristics. Section IV applies this technique/equation to obtain a large-signal model of a $10 * 140$ μm GaAs-MESFET chip (F20 bathtub process) from the GEC- Marconi Foundry and a $16 * 250$ μm MESFET chip (DIOM process) from the Siemens Foundry, extracted from experimental dc, pulsed, and S parameters. The breakdown effect has not been modeled because it is not the focus of this work. MDS simulations based on the model of the equation were compared with experimental measurements of the transistor charged by 50 Ohms at the input and output ports. The agreement between the simulations and the experimental results was found to be very good.

II. Description of Phenomena Involved in Pulsed Behavior of GaAs-MESFET's

Several authors [8]–[10] have demonstrated the importance of nonlinear characterization of transistors from pulsed *I/V* measurements. Therefore, it is necessary to develop pulsed nonlinear models capable of taking into account phenomena such as low-frequency dispersion (associated with deep level traps and surface state densities in GaAs-MESFET's [11]) and

Manuscript received July 11, 1994; revised November 27, 1995. This work was supported in part by the European ESPRIT project—MANPOWER—6050, the TIC-1020/92-C02-01, and TIC-672/93-C04-04 Spanish CICYT projects.

The authors are with the Universidad de Cantabria, Departamento de Electronica, 39005 Santander, Spain

Publisher Item Identifier S 0018-9480(96)01541-4

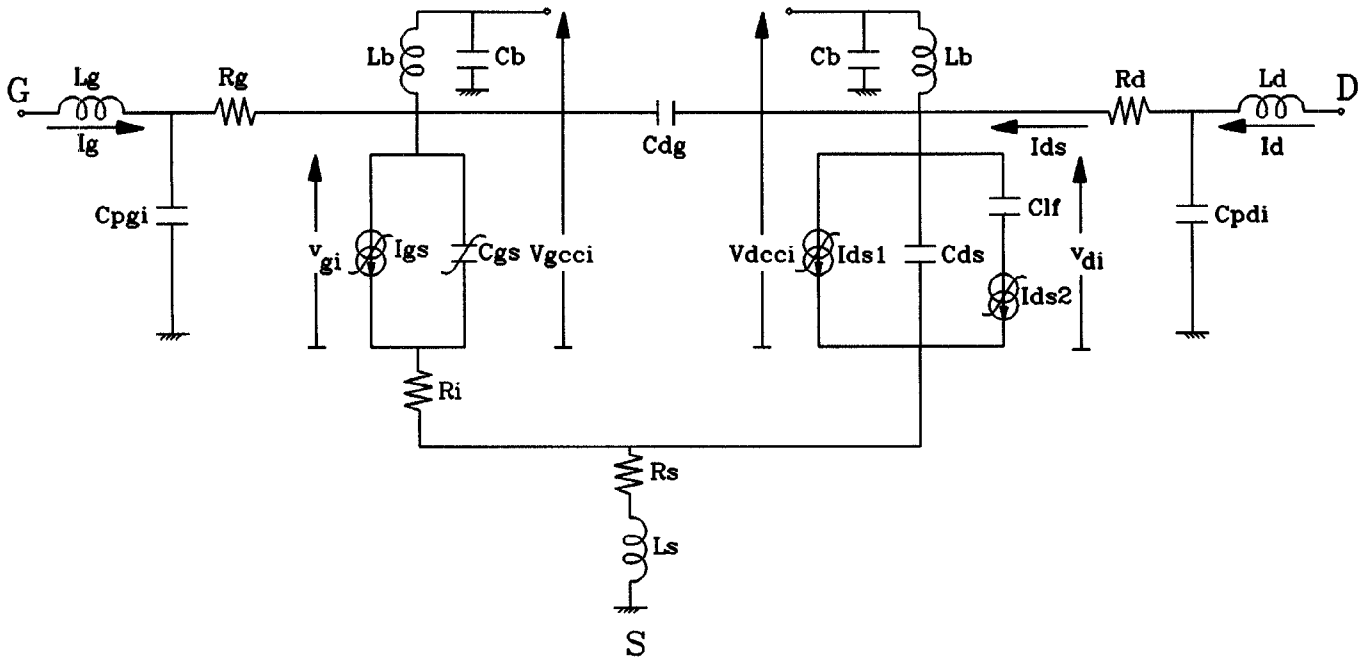

Fig. 1. GaAs MESFET equivalent circuital model.

thermal effects as well as dc, pulsed, and RF operation. The following phenomena are involved in the large signal behavior of the GaAs-MESFET transistors.

1) Trapping Effects and Surface States: From a macroscopic point of view, these phenomena provoke low-frequency dispersion (from dc to some hundreds of KHz) of the transconductance and output conductance [9], [11]. This behavior leads to significant problems when both dc and RF operation must be modeled. The influence of these effects on the pulsed characteristics is negligible because they have ionization and recombination time constants from microseconds to milliseconds, while the pulse rise time used to obtain the I_{ds} characteristics is about 50 nS and the duty cycle is around 1/1000. Therefore, these phenomena have been included in the CAD-oriented circuit model of Fig. 1 [10], [12]. They are represented by the current source I_{ds2} and the C_{lf} capacitor.

2) Operating-Point Dependence: The variations in the pulsed *I/V* characteristics with the quiescent point are well known [9], but it is very important to separate the different phenomena that induce these variations in pulsed operation. From a macroscopic point of view, assuming that the ambient temperature remains constant, two main effects can be distinguished. The first is caused by the self-heating at each operating point, assuming that this variation depends only on the average dissipated power $P_0 = \frac{1}{T}\int_a^b v_D(t) \cdot i_D(t)dt$ [11].

The second effect is due to the variation in channel resistance as a function of gate and drain voltages. Fig. 2 shows the variations in experimental pulsed characteristics when there is no dissipated dc power (i.e., $V_{dscc} = 0$). In this case, the variations are caused by the different channel widths of the transistor. Fig. 3 shows pulsed curves for constant dc power at different quiescent points with $V_{dscc} \neq 0$ and it can be seen that there are significant differences. Since it is impossible to separate these two effects, a bias-dependent equation is needed to reproduce the nonlinear pulsed behavior.

Since the thermal time constant of GaAs-MESFET's is on the order of a few microseconds, the pulsed measurements were made maintaining the transistor at each operating point for several seconds in order to keep the operation temperature constant. The pulsed *I/V* measurement system (PIVMS) used is a high-speed automated setup controlled internally by one main mathematical controller and two internal microprocessors for gate and drain ports. This system permits control of the frequency, the rise time, and the width of the pulses [14].

III. Operating-Point-Dependent Nonlinear Model for MESFET's

Considering the effects described above, we have developed a nonlinear double current source model of I_{ds}. If the dc and pulsed characteristics are known at a few bias points, this model reproduces the I_{ds} current behavior at any operation point.

Fig. 1 shows the total nonlinear GaAs-MESFET model. V_{gcci} and V_{dcci} are the internal values of the external operation point (V_{gscc}, V_{dscc}), while v_{gi} and v_{di} are the internal instantaneous voltages. C_b and L_b are typical parameters of a low pass filter used to obtain the intrinsic dc dependence. C_{lf} is a linear capacitor and it contributes to simulate the low-frequency dispersion. Its value can be obtained from low-frequency RF measurements (from dc to beyond cut off frequency).

Considering the circuit of Fig. 1, we can write I_{ds} as an analytical function of I_{ds1} and I_{ds2}

$$I_{ds}(v_{gi}, v_{di}, V_{gcci}, V_{dcci}) = I_{ds1}(v_{gi}, v_{di}) + I_{ds2}(v_{gi}, v_{di}, V_{gcci}, V_{dcci}).$$

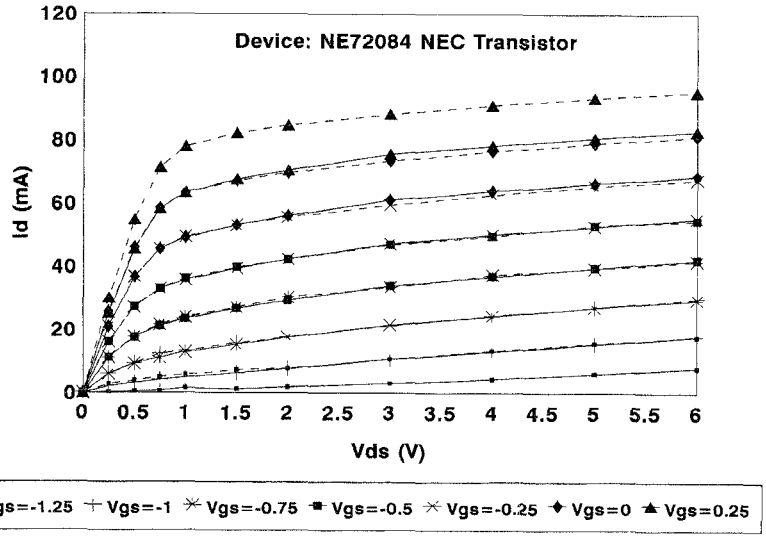

Fig 2. Variations of experimental pulsed curves when dissipated dc power does not exist ($V_{\mathrm{dscc}} = 0$). Solid lines: $V_{\mathrm{gscc}} = -1$. Dashed lines: $V_{\mathrm{gscc}} = -0.5$.

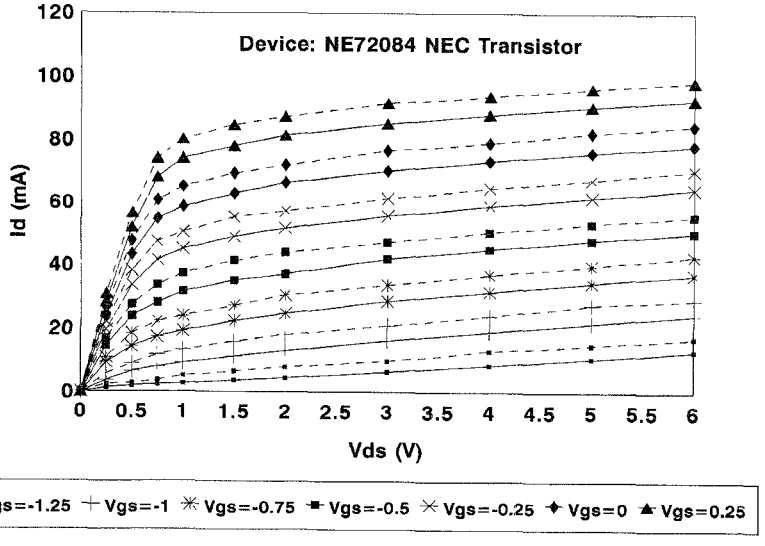

Fig 3 Variations of experimental pulsed curves for constant dc power at two different bias points when $V_{\mathrm{dscc}} \neq 0$. Solid lines: $V_{\mathrm{gscc}} = -0.75$, $V_{\mathrm{dscc}} = 3$. Dashed lines. $V_{\mathrm{gscc}} = 0$, $V_{\mathrm{dscc}} = 1$.

$I_{\mathrm{ds1}}(v_{\mathrm{g1}}, v_{\mathrm{d1}})$ represents the dc characteristics of the transistor, which have been modeled using the Materka equation [16].

$I_{\mathrm{ds2}}(v_{\mathrm{g1}}, v_{\mathrm{d1}}, V_{\mathrm{gcc1}}, V_{\mathrm{dcc1}})$ takes into account the dependence on the instantaneous voltages $(v_{\mathrm{g1}}, v_{\mathrm{d1}})$ and the internal operating point.

The total equation is given by (1)

$$I_{\mathrm{ds}} = I_{\mathrm{dss}}(V_{\mathrm{gcc1}}, V_{\mathrm{dcc1}}) \times \left(1 - \frac{v_{\mathrm{g1}}}{V_t(V_{\mathrm{gcc1}}, V_{\mathrm{dcc1}}) + \gamma(V_{\mathrm{dcc1}})v_{\mathrm{di}}}\right)^{(\mu+\delta v_{\mathrm{g1}})} \times (1 + \lambda(V_{\mathrm{gcc1}}, V_{\mathrm{dcc1}})v_{\mathrm{d1}}) \cdot \tanh\left(\frac{\alpha(V_{\mathrm{gcc1}}, V_{\mathrm{dcc1}})}{I_{\mathrm{dss}}} v_{\mathrm{di}}\right). \quad (1)$$

The multibias nonlinear (1) is based on the Materka equation. It has six parameters: $I_{\mathrm{dss}}, V_t, \gamma$, and λ are bias-dependent parameters whereas μ and δ are constant for each transistor.

The parameter I_{dss} is the most influential one in the equation because it multiplies the rest of the equation and it has a very high value. This means that small variations in the rest of the parameters result in large variations in the current value of the equation. Of course, this effect is more important in power MESFET transistors. However, the model smooths this effect by using the parameter I_{dss} to control the slope of the linear part of the characteristics. The variation in I_{dss} with the operating point is given by

$$I_{\mathrm{dss}} = \frac{\beta}{|V_{\mathrm{gcc1}} - 1|^p (1 + V_{\mathrm{dcc1}})^q} \quad (2)$$

where V_{gcc1} and V_{dcc1} are the independent voltages corresponding to the operating point $(V_{\mathrm{gscc}}, V_{\mathrm{dscc}})$ being considered. The exponents p and q are independent parameters of the quiescent point and β is a function of V_{gcc1} and V_{dcc1}. This function takes into account two phenomena: one of them is the change in the average dissipated dc power (self-heating) with

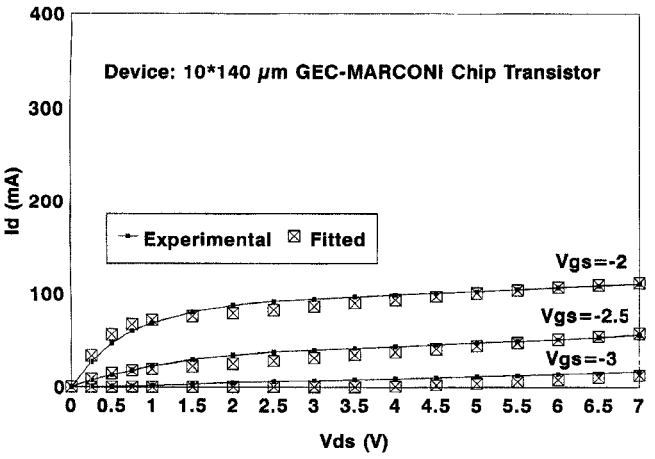

Fig. 4. Fitting of the pinch-off region using the new I_{ds} proposed equation. Pulsed curves from the operating point $(-1, 3)$.

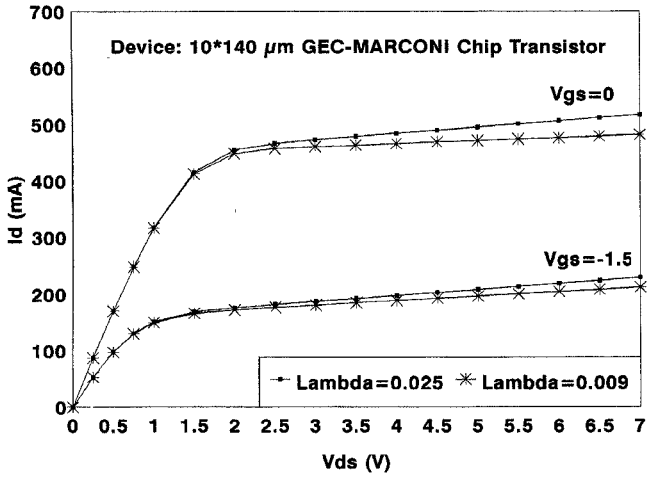

Fig. 5. Simulations of the *I/V* pulsed curves dependence on the value of λ parameter.

the operating point [11], and the other one is the variation in channel resistance. Figs. 2 and 3 show the variation in $I_{\rm dss}$ when $V_{\rm dscc} = 0$ and $V_{\rm gscc} \neq 0$. β is a function of the independent variables $V_{\rm gcci}$ and $V_{\rm dcci}$

$$\beta = \beta_0 V_{\rm gcci} + \beta_1 + ((\beta_2 V_{\rm gcci} + \beta_3) V_{\rm dcci})^{\beta_4}. \quad (3)$$

Returning to (1), the parameter V_t represents the pinch-off behavior, which is very common in nonlinear modeling [16], [17]. Analyzing the term that controls the pinch-off region in (1), we can see that it is dependent on $v_{\rm gi}$ through the parameter γ. This means that the model is capable of predicting accurately the very low current zone (Fig. 4). For this reason, the operating-point variations of the parameters V_t and γ have been studied together. The following function is proposed to represent the variation in V_t

$$V_t = V_{t_0} V_{\rm gcci} + (V_{t_1} V_{\rm dcci} + V_{t_2}). \quad (4)$$

The pinch-off behavior resulting from variations in $V_{\rm dcci}$ are corrected by using the parameter γ

$$\gamma = \gamma_0 + \gamma_1 \sqrt[\gamma_2]{V_{\rm dcci}}. \quad (5)$$

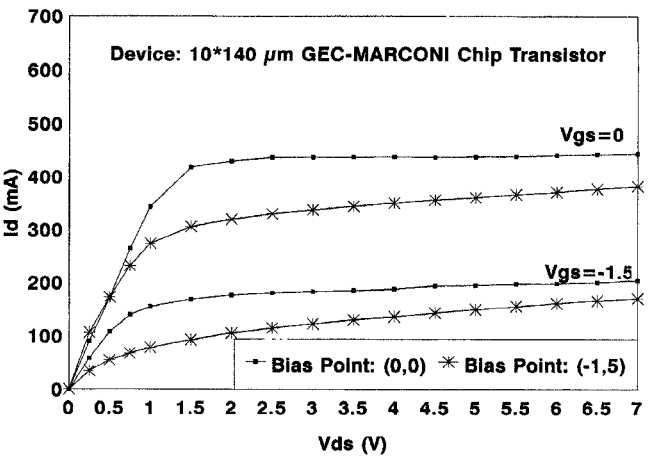

Fig. 6. *I/V* pulsed curves dependence of the linear region on the operating point (α variations).

TABLE I
VALUES OF THE DIFFERENT KEY POINTS

Point	V_{gs}	V_{ds}
P1	$V_{gscc}=V_{gs}(I_{dss})$	0
P2	$V_{gscc}=V_{gs}(I_{dss}/2)$	0
P3	$V_{gscc}=V_{gs}$(Pinch-Off)	0
P4	$V_{gscc}=V_{gs}(I_{dss})$	$V_{dscc}=V_{ds}$max
P5	$V_{gscc}=V_{gs}$(Pinch-Off)	$V_{dscc}=V_{ds}$max
P6	$V_{gscc}=V_{gs}(I_{dss}/2)$	$V_{dscc}=V_{ds}$max/2

Equations (4) and (5) reproduce the behavior of the transistor in the low-current region, not only as a function of the independent variables $(v_{\rm gi}, v_{\rm di})$, but also of the operating point. This provides excellent results as can be seen, for instance, in Fig. 4.

The factor $(1 + \lambda \cdot v_{\rm di})$ in (1) mainly reproduces the output conductance function of the instantaneous voltage at the drain terminal, and λ, which has the dimensions of conductance, is principally responsible for the slope of the $I_{\rm ds}$ curves in the saturation region.

In Fig. 5 it can be observed that changes in λ result in significant variations in the slope in the saturation zone (output conductance) of the pulsed characteristics (RF and pulsed operation). The variation law of this parameter is given by

$$\lambda = \lambda_0 + \lambda_1 V_{\rm gcci} + \lambda_2 V_{\rm gcci}^2 + \lambda_3 V_{\rm dcci} + \lambda_4 V_{\rm dcci}^2. \quad (6)$$

The parameter α in the hyperbolic tangent term of (1) controls the linear region. The difference with respect to other models [17] is that the argument of the hyperbolic tangent contains α divided by the parameter $I_{\rm dss}$.

Fig. 6 shows the variations in the linear zone of the pulsed characteristic curves at different operating points. For instance, pulsed curves at operating points near to $V_{\rm gscc} = 0$ and $V_{\rm dscc} = 0$ have higher gradients in the linear zone than characteristic curves at $V_{\rm dscc}$ in the saturation region and $I_{\rm dss}/2$. The variation of the parameter α is given by

$$\alpha = \alpha_0 + \alpha_1 V_{\rm gcci} + \alpha_2 V_{\rm gcci}^2 + \alpha_3 V_{\rm dcci} + \alpha_4 V_{\rm dcci}^2. \quad (7)$$

TABLE II
VALUES FOR THE PARAMETERS OF THE COMPLETE NONLINEAR MODEL FOR A $10 * 140$ μm GEC-MARCONI CHIP TRANSISTOR

Linear Parameters				
R_g (Ohm): 3.27	R_d (Ohm): 1.08	R_s (Ohm): 0.87	L_g (nH): 0.102	L_d (nH): 0.049
L_s (nH): 0.006	L_d (nH): 0.097	C_{ds} (pF): 0.37	C_{pg1} (pF): 0	C_{pd1} (pF): 0
R_i (Ohm): 3.27	C_{if} (pF): $1*10^6$	Transit time (ps): 3.5		
Non-linear Parameters				
C_{gs} Schottky	C_{gso} (pF): 1.801	γ: 0.5	V_{bi} (Volt): 0.47	
I_{gs} Schottky	α_s: 30.58	I_{ns}: $0.1025*10^{-10}$	I_{dg} Linear	R_{dg}(Ohm): $1*10^{10}$
I_{ds1} DC (Materka)	I_{dss}: 0.4458	V_t: -2.577	γ: -0.1089	E: 1.270
	K_c: -0.05288	S_s: $-0.7663*10^{-2}$	S_i: 1.927	K_g: 0.4495
I_{ds} PULSED (Our Model)	μ: 1.337	δ: $-0.2178*10^{-1}$	p: 0.14	q: 0.29
	β_0: -11.73	β_1: 517.9	β_2: -41180	β_3: 10850
	β_4: .3843	V_{t0}: $-0.7012*10^{-1}$	V_{t1}: $-0.925*10^{-1}$	V_{t2}: -2.819
	γ_0: -0.07893	γ_1: -0.03537	γ_2: 1.892126	λ_0: $-0.3264*10^{-2}$
	λ_1: $-0.7271*10^{-2}$	λ_2: $-0.6534*10^{-3}$	λ_3: $1.267*10^{-2}$	λ_4: $-0.1112*10^{-2}$
	α_0: 1.506	α_1: 0.1921	α_2: 0.02383	α_3: -0.04551
	α_4: $0.1695*10^{-4}$			

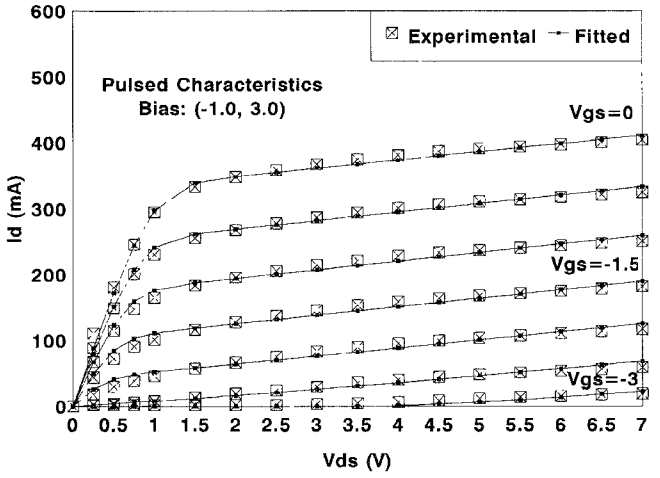

Fig. 7 Experimental and fitted *I/V* pulsed curves at $(-1\ 3)$ operating point for a $10 * 140$ μm GEC-MARCONI device

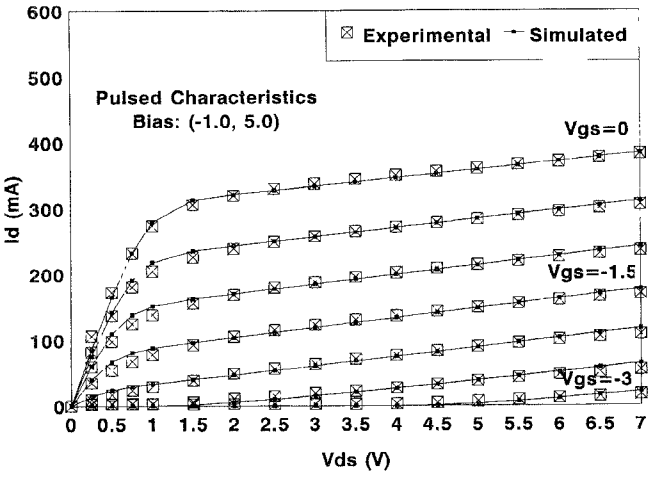

Fig. 8. Experimental and simulated *I/V* pulsed curves at $(-1, 5)$ operating point for a $10 * 140$ μm GEC-MARCONI device.

The equations obtained to represent the different parameters of (1) have been used to model transistors of different technologies and sizes giving good results in all cases. Comparisons with experimental results will be presented in the next section.

IV. SIMULATIONS AND EXPERIMENTAL RESULTS

Equation (1) reproduces the pulsed characteristic curves at any quiescent bias point. To extract the different parameters of the equation $I_{\rm ds}$, pulsed measurements must be considered at six key operating points. These key points have been selected so that the influence of the polarization on the parameters of the equation is taken into account. Table I indicates the values of the key points on typical dc characteristic curves.

P_1, P_2, and P_3 take into account the influence of the different channel widths of the transistor and allow us to study how the parameters of (1) vary with this effect (average dissipated power $P_0 = 0$). Using this method, it was found that the parameter γ does not vary with $V_{\rm gscc}$, which is to be expected because γ corrects the pinch-off effect only with the $V_{\rm dscc}$ voltage. Points P_4, P_5, and P_6 take into account the variations with the self-heating of the transistor ($I_{\rm dscc} \neq 0$). Fig. 7 shows, as an example, the experimental and fitted pulsed curves at a particular key point.

The parameters of the nonlinear function $I_{\rm ds1}(v_{\rm gi}, v_{\rm di})$ have been extracted by means of experimental measurement of the dc characteristics. The access resistors R_g, R_s, andR_d (Fig. 1) and the typical Schottky current parameters $I_{\rm ns}$ and α_s [18] have been obtained from dc measurements by three different

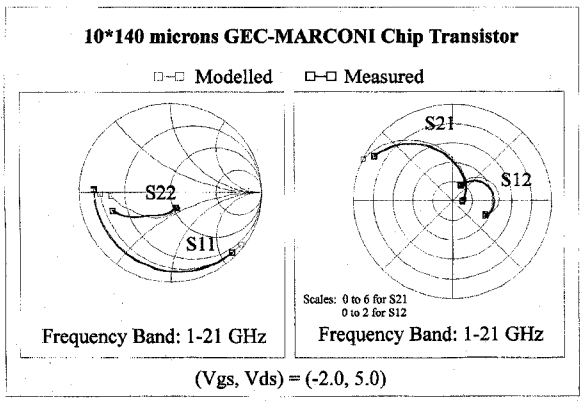

Fig. 9. Experimental and simulated S parameters using the complete nonlinear model for a $10 * 140$ μm GEC-MARCONI device.

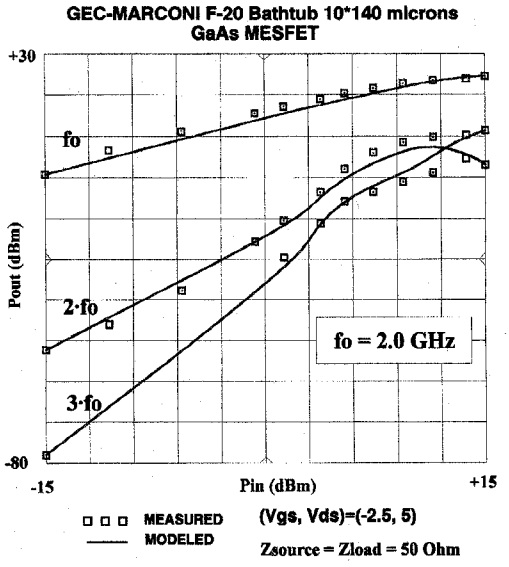

Fig. 10. Experimental and simulated $P_{\text{in}}/P_{\text{out}}$ behavior of the transistor using the complete nonlinear model for a $10 * 140$ μm GEC-MARCONI device.

methods [16], [19], and [20]. The rest of the linear elements of the circuit shown in Fig. 1 along with the parameters of the nonlinear capacitors C_{gs} and C_{dg} have been obtained from S parameter measurements using hot and cold device techniques together with multibias linear extractions, minimizing the error function by optimization [9], [18], and [20].

In order to validate our equation, a complete nonlinear model has been extracted for a $10 * 140$ μm MESFET chip (F20 Bathtub process) from GEC-MARCONI, which is given in Table II. Fig. 8 compares pulsed measurements with simulations by (1). It can be seen that the operating point is very different from the fitted key points. This demonstrates that the model is capable of reproducing the variations in the pulsed behavior with the quiescent operating point.

The total large signal MESFET equivalent circuit has been implemented in the MDS nonlinear simulator. Fig. 9 shows the agreement of the RF small signal behavior in the frequency band. Fig. 10 shows that there is very good agreement between simulations and experimental results of the output power versus the input power of the first three harmonics of the device of Table II, loaded by 50 Ohms at the input and output

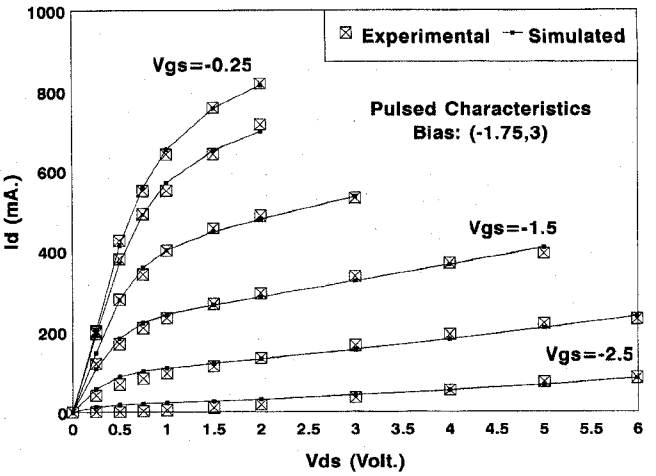

Fig. 11. Experimental and simulated *I/V* curves at $(-1.75, 3)$ bias point for a $16 * 250$ μm Siemens device.

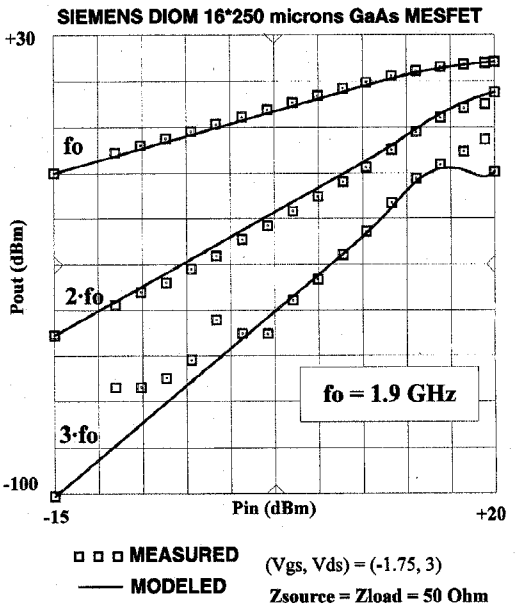

Fig. 12. Experimental and simulated $P_{\text{in}}/P_{\text{out}}$ behavior using the complete nonlinear model for a $16 * 250$ μm Siemens device.

ports at 2 GHz and a bias point of $(-2.5, 3)$. The $P_{\text{out}}/P_{\text{in}}$ measurements have been made using a HP8341B Synthesized Sweeper and a HP438A Power Meter with two HP8485A Power Sensors (attenuation accuracy $+\backslash -3\%$).

Using the same methodology we have modeled a $16 * 250$ μm MESFET chip (DIOM process) from Siemens. Fig. 11 shows the experimental and simulated pulsed curves and the $P_{\text{out}}/P_{\text{in}}$ behavior is shown by Fig. 12. The power measurements of this transistor were carried out by IMST Co. of Germany.

V. Conclusion

This paper analyzes some hypotheses about phenomena such as low-frequency dispersion (associated with deep level traps and surface state densities in GaAs-MESFET's) and thermal effects as well as dc, pulsed, and RF operation. As a consequence of this study, a suitable nonlinear equation has been developed for the current source I_{ds} which is

capable of taking into account the operating point dependence. I_{ds1} reproduces the dc behavior and I_{ds2} represents the RF operating-point dependence. Experimental measurements of the pulsed characteristics and simulations have been performed for different kinds of transistors. Excellent agreement was observed between MDS simulations using this model and power measurements for two chip transistors ($10 * 140$ μm from GEC-MARCONI and $16 * 250$ μm from Siemens) loaded by 50 ohms at the input and output ports.

REFERENCES

[1] C. Raucher and H. A. Willing, "Simulation of nonlinear microwave FET performance using a quasi-static model," *IEEE Trans. Microwave Theory Tech.*, vol. MTT-27, no. 10, Oct. 1979.

[2] H. Sledzik and I. Wolff, "Large signal modeling and simulation of GaAs MESFET's and HFET's," *Int. J. Microwave M.-W. Comp.-Aided Eng.*, vol. 2, no. 1, pp. 49–60, 1992.

[3] H. Kondoh, "An accurate FET modeling from measured S-parameters," in *IEEE MTT Symp. Dig.*, June 1986, pp. 377–380.

[4] M. Paagi, P. H. Williams, and J. M. Borrego, "Nonlinear GaAs MESFET modeling using pulsed gate measurements," in *IEEE MTT Symp. Dig.*, 1988, pp. 229–231.

[5] J. F. Vidalou, F. Grossier, M. Camiade, and J. Obregon, "On wafer large signal pulsed measurements," in *IEEE MTT Symp. Dig.*, 1989, pp. 831–834.

[6] J. M. Golio, M. Miller, G. N. Maracas, and D. A. Johnson, "Frequency dependent electrical characteristics of GaAs MESFET," *IEEE Trans. Electron Dev.*, vol. 37, May 1990.

[7] N. Scheinberg, R. Bayruns and R. Goyal, "A low-frequency GaAs MESFET circuit model," *IEEE J. Solid-State Circuits*, vol. 23, pp. 605–608, Apr. 1988.

[8] A. Platzker, A. Palevsky, S. Nash, W. Struble, and Y. Tajima, "Characterization of GaAs devices by a versatile pulsed *I-V* measurement system," in *IEEE MTT Symp. Dig.*, 1990, pp. 1137–1140.

[9] T. Fernández, A. Mediavilla, A. Tazón, and J. L. García "Low frequency dispersion measurements for nonlinear microwave MESFET modeling," in *GaAs'92 Eur. Gallium Arsenide Symp., ESTEC*, Noordwijk, The Netherlands, Apr. 1992.

[10] T. Fernández, Y. Newport, J. M. Zamanillo, A. Tazón, and A. Mediavilla, "Modeling of operating point non linear dependence of I_{ds} characteristics from pulsed measurements in MESFET transistors," in *23rd European Microwave Conf.*, Madrid, Sept. 1993, pp. 518–521.

[11] F. Filicori, G. Vanini, A. Mediavilla, and A. Tazón, "Modeling of deviations between static and dynamic drain characteristics in GaAs FET's," in *23rd Eur. Microwave Conf.*, Madrid, Sept. 1993, pp. 454–457.

[12] A. Mediavilla, A. Tazón, and J. L. García, "Phenomena description of pulsed characterization of GaAs-MESFET transistors for nonlinear modeling purposes," in *GAAS 94, Applicat. Symp.*, Apr. 1994, pp. 415–418.

[13] L. Selmi and B. Riccò, "Modeling temperature effects in the DC *I-V* characteristics of GaAs MESFET's," *IEEE Trans. Microwave Theory Tech.*, vol. 40, no. 2, Feb. 1993.

[14] T. Fernández, Y. Newport, J. M. Zamanillo, A. Mediavilla, and A. Tazón, "High speed automated pulsed *I/V* measurement system," in *23rd European Microwave Conf.*, Madrid, Sept. 1993, pp. 494–496.

[15] T. J. Brazil, "A universal large-signal equivalent circuit model for the GaAs MESFET," in *21st European Microwave Conf.*, Sept. 1991, pp. 921–926.

[16] T. Kacprzak and A.Materka, "Compact DC model of GaAs-FET's for large signal computer calculation," *IEEE J. State Solid Circuits*, vol. SC-18, pp. 211–213, Apr. 1983.

[17] W. Curtice, "A MESFET Model for use in the design of GaAs integrated circuits," *IEEE Trans. Microwave Theory Tech.*, vol. MTT-28, no. 5, pp. 448–456, May 1980.

[18] J. L. García, A. Tazón, and A. Mediavilla, "Non linear modeling techniques of high frequency MESFET transistors," in *Proc. 1993 SBMO Int. Microwave Conf.*, Sao Paulo, Brazil, Aug. 1993, pp. 605–616.

[19] T. Fernández, Y. Newport, A. Tazón, and A. Mediavilla, "Extracting advanced large signal MESFET models from DC, AC and pulsed *I/V* measurements," in *MIOP '93*, Sindelfingen, Germany, May 1993, pp. 472–475.

[20] H. Fukui, "Determination of the basic parameters of a GaAs MESFET," *Bell Syst. Tech. J.*, vol. 58, no. 3, pp. 772–797, 1879.

Tomás Fernández was born in Torrelavega, Spain, in 1966. He received the "Licenciado" degree in physics from the University of Cantabria, Spain, in 1990.

Since then he has been with the Electronics Department at the same university, where he is working toward the Doctor degree in physics. His research interests include nonlinear modeling of GaAs MESFET's and HEMT's.

Yolanda Newport was born in Rotterdam, The Netherlands, in 1964. She received the "Licenciado" degree in physics from the University of Cantabria, Spain, in 1989.

Since then she has been with the Electronics Department at the same university, where she is currently an Associate Professor and is working toward the Doctor degree in physics. Her research interest include nonlinear modeling of GaAs MESFET's and HEMT's.

José M. Zamanillo was born in Madrid, Spain, in 1963. He received the "Licenciado" degree in physics from the University of Cantabria, Spain, in 1988.

Since then he has been with the Electronics Department at the same university, where he is currently an Associate Professor and is working toward the Doctor degree in physics. His research interests include linear and nonlinear modeling of GaAs MESFET's and HEMT's.

Antonio Tazón (M'92) was born in Santander, Spain, in 1951. He graduated in 1978 and received the Doctor of Physics degree in 1987, both from the University of Cantabria, Santander, Spain.

Since 1991 he has been a Professor in the Department of Electronics of the University of Cantabria. He has worked in analysis and optimization of nonlinear microwave active devices and circuits in both hybrid and monolithic tecnologies, and currently, he is working on active microwave circuits, mainly in the area of nonlinear modeling of GaAs devices and their applications in large-signal computer design.

Angel Mediavilla (M'92) was born in Santander, Spain, in 1955. He graduated (with honors) in 1978 and received the Doctor of physics degree in 1984, both from the University of Cantabria, Santander, Spain.

From 1980 to 1983 he was Ingénieur Stagière at Thomson-CSF, Corbeville, France. He is currently Professor in the Department of Electronics of the University of Cantabria. He has wide experience in analysis and optimization of nonlinear microwave active devices and circuits in both hybrid and monolithic tecnologies. His current research fields are on active microwave circuits, mainly in the area of nonlinear modeling of GaAs devices and their applications in large-signal computer design.